Appl Phys B (2010) 99: 817–823
DOI 10.1007/s00340-010-3986-x

**Applied Physics B**
**Lasers and Optics**

# On the influence of bimodal size distributions in particle sizing using laser-induced incandescence

**J. Johnsson · H. Bladh · P.-E. Bengtsson**

Received: 23 October 2009 / Revised version: 18 January 2010 / Published online: 17 March 2010


**Abstract** Time-resolved laser-induced incandescence (LII) is a technique for in-situ soot particle size distribution measurements with the limitation that the distribution function has to be assumed (often monodisperse or lognormal) in the signal analysis. Since it is established that size distributions sometimes are bimodal, it is of interest to understand the influence from such distributions on the LII signal, and consequently what information can be extracted from experimental LII signals. The influence of the parameters of the bimodal lognormal distribution on the evaluation using a monodisperse or lognormal distribution was investigated. A range of bimodal distributions were tested and it was found that a unimodal evaluation of a signal from a bimodal distribution is only slightly affected by its small-size mode, meaning that LII can be used to determine the approximate parameters of the large-size mode.

## 1 Introduction

Laser-induced incandescence (LII) is a diagnostic method for remote measurements of soot properties within hot reactive gases as well as in cold flows, such as in the gases of a combustion process and in its exhausts [1, 2]. Although the method was proposed and demonstrated already in the 1970s [3, 4], it has been most actively developed during the last 15 years for measurements of soot volume fractions and particle sizes [5–13]. The basic principle of LII is that soot particles are heated by a short laser pulse to temperatures of 3500–4000 K, and the subsequent increased blackbody radiation from the particles is analyzed in terms of volume fractions and/or sizes. The time-resolved LII signal can be analyzed in terms of particle size, since the cooling of the soot particles proceeds with different rates depending on their sizes. The evaluation is performed using a heat and mass transfer model for the laser-heated particles [14–16]. LII has proven to be useful in fundamental studies as well as in applied measurements, but there are still a number of issues that need to be addressed to improve the understanding of the fundamental processes and thereby also the accuracy of the evaluated soot properties.

Although particle sizing using LII was discussed and demonstrated already by Weeks and Duley in 1974 [3], it was not until the studies by Will et al. [17, 18] and Roth and Filippov [19] in the middle of the 1990s that LII demonstrated its potential for soot particle sizing in flames. In these studies, a monodisperse size distribution was assumed and evaluated. However, soot particle distributions generally consist of a range of different particle sizes, and the lognormal size distribution has been shown to be a good approximation for various flame conditions, see for example [20–24]. Evaluation of both the shape and position of a size distribution from an LII signal is a challenging task, which is why the distribution is often fixed to a lognormal shape, leaving two parameters to fit: the geometric mean diameter, $d_g$, and the geometric standard deviation, $\sigma_g$. Even when such a parameterized distribution is assumed, the analysis can be cumbersome, since the minimum in the least-squares fit procedure is shallow in the parameter space spanned by $d_g$ and $\sigma_g$, which has been discussed

J. Johnsson (✉) · H. Bladh · P.-E. Bengtsson
Division of Combustion Physics, Lund University, P.O. Box 118, 221 00 Lund, Sweden
e-mail: jonathan.johnsson@forbrf.lth.se
Fax: +46-46-2224542

H. Bladh
e-mail: henrik.bladh@forbrf.lth.se

P.-E. Bengtsson
e-mail: per-erik.bengtsson@forbrf.lth.se

thoroughly in [12]. Also, a lognormal size distribution may not always be the best assumption. In a recent investigation of LII signals recorded from measurements in a Diesel engine, it was shown that a theoretically calculated LII signal from a multi-lognormal distribution agreed better with an experimental LII signal than that from a single-lognormal distribution [25].

An important aspect in the evaluation of a size distribution from an LII signal is that the signal is relatively insensitive to the smaller particles of the distribution. The main reason for this is that the radiation from soot particles in the Rayleigh regime, in which particle sizes are much smaller than the wavelengths [26], is proportional to the particle volume when the particles have the same temperature. Also contributing to the insensitivity is the fact that the approximately exponential cooling rate is larger for the smaller particles, because of their larger surface to volume ratio. Since the LII signal is stronger for particles with higher temperature ($\sim T^5$, where $T$ is the absolute temperature) this difference in cooling rate leads to a decreased sensitivity of the LII signal to smaller particles. This means, that not only do the smaller particles have a much smaller contribution to the LII signal when all particles are heated to the same temperature by the laser pulse, but also that their relative contribution becomes successively smaller as the particles cool.

In addition to the investigations where lognormal distributions have been observed, several studies during the last decade have found soot size distributions in flames to sometimes be bimodal [27–29]. Abid et al. [29] made measurements in a premixed ethylene/oxygen/argon flame, stabilised on a sintered porous plug burner, using a scanning mobility particle sizer (SMPS). The measurements were made for different flame temperatures and at different heights above burner, and some of the experimental cases showed bimodal distributions. Stirn et al. [27] also used an SMPS to measure soot particle size distributions in ethylene/air flames on a stainless-steel McKenna burner, at a number of heights above the burner (HAB) and equivalence ratios, $\Phi$. For some conditions, the measured size distributions were bimodal, also at heights where aggregation has not yet become dominant. A general question thus arises, and that is to what extent the mode with small sizes (from now on called the small-size mode) of a bimodal distribution influences the evaluation of the size distribution. Although this topic has been partially treated in other studies [2, 30], in this work we present a theoretical investigation of how various parameters of a bimodal distribution influence the evaluated particle size distribution. It is shown that for some cases the evaluated size distribution closely resembles the large-size mode of the bimodal distribution. Moreover, the influence of the start time of the signal analysis on the evaluated particle size distribution is investigated.

## 2 LII model and evaluation procedure

The LII model that is used for the evaluation of all LII signals in this work is the one described in Bladh et al. [16], with the modifications that the sublimation sub-model is turned off, since the particle temperature never exceeds 3600 K. The laser pulse heating and subsequent cooling of the soot particles is described in the model using heat and mass balance equations. The particles are assumed to be graphite-like and hence values of material constants associated with graphite are used. As a consequence, the small-size mode and the large-size mode of a bimodal distribution are assumed to consist of particles with the same properties in the analysis in the present work. When applying this analysis to a real bimodal distribution in the soot growth region of a flame, it should be noticed that especially the small-size mode may have significantly different properties. The implication of this is discussed in Sect. 3.4.

The experimental parameters used in the model are similar to those used in Bladh et al. [23]: The laser pulse at 1064 nm is a spatial tophat with a Gaussian time profile (FWHM = 10 ns). The laser fluence is 0.12 J/cm$^2$ and the signal is detected at 575 nm. The particle size distributions that are used in the model are discretised with a step size of 0.05 nm for the diameters. The heat accommodation, $\alpha_T$, was set to 0.3 and the absorption function $E(m)$ was set to 0.4, which are within the spans of values from recent investigations [2]. As will be discussed later, the sensitivity on the presented results from these parameters was marginal.

The evaluations of particle sizes from LII signals were made according to the procedure in Bladh et al. [23]. The least-squares fit of a modeled signal to the simulated experimental signal is made from 20 ns after the signal peak until the end of the signal at 900 ns after the peak, unless otherwise stated, and the two signals are normalised at the start of the evaluation interval.

When using LII to evaluate primary particle sizes, some assumptions need to be made regarding the shape of the size distribution. One of the most common parameterized distributions that have been used in evaluations is the lognormal distribution, which has been shown to describe soot particle distributions reasonably well [20–24]. To find $d_g$ and $\sigma_g$ of a lognormal distribution in a fit to an LII signal created from a lognormal distribution is a mathematically ill-posed problem [12]. There is, however, a unique solution to the problem, and it has been shown that there is just one minimum in the residual ($\chi^2$) surface of the fit, making it straightforward to find the solution using a least-squares fitting algorithm [12]. A residual surface was calculated for the case where modeled signals from lognormal distributions were fitted to a signal from a modeled bimodal lognormal distribution. This surface was found to have a shape similar to that of the residual surface described above. This indicates that

**Table 1** Case A: Parameters for bimodal lognormal distributions similar to those acquired by Stirn et al. [27] in an ethylene/air flame on a stainless-steel McKenna burner at $\Phi = 2.1$ and HAB = 10 mm. The weight of the large-size mode has been normalized to $w_2 = 1$. $d_{g1}$ and $d_{g2}$, $\sigma_{g1}$ and $\sigma_{g2}$, and $w_1$ and $w_2$ are the geometric mean particle diameters, the geometric standard deviations, and the weights of the small-size mode, $p_1$, and the large-size mode, $p_2$, respectively. Case B: A range of cases where the large-size mode is fixed and the small-size mode weight and geometric diameter are varied

| Case | $w_1$ | $d_{g1}$ [nm] | $\sigma_{g1}$ | $w_2$ | $d_{g2}$ [nm] | $\sigma_{g2}$ |
|---|---|---|---|---|---|---|
| A | 0.75 | 4.2 | 1.23 | 1.0 | 11.1 | 1.34 |
| B | 0–10 | 3.0–11.0 | 1.3 | 1.0 | 11.0 | 1.3 |

this problem is similar: it is ill-posed but has a unique solution, and there are no local minima in the residual surface that can cause problems for the fitting routine.

To assess the influence of the small-size mode on the evaluation of an LII signal, a bimodal lognormal size distribution is created. The parameters of the distribution are similar to those in a distribution presented by Stirn et al. [27], acquired using an SMPS from ethylene/air flames on a stainless-steel McKenna burner at an equivalence ratio ($\Phi$) of 2.1 and a height above burner (HAB) of 10 mm. This case was chosen since our measurements at similar conditions [23] suggest that the particles in this distribution are mostly non-aggregated, making it reasonable to assume that also the SMPS sizes mainly correspond to isolated particles. The parameters of this distribution are shown in Table 1, case A. The bi-lognormal distribution, $p_b$, is given by

$$
\begin{aligned}
p_b(d) &= w_1 p_1(d) + w_2 p_2(d) \\
p_1(d) &= p_n(d, d_{g1}, \sigma_{g1}) \\
p_2(d) &= p_n(d, d_{g2}, \sigma_{g2}) \\
p_n(d, d_g, \sigma_g) &= \frac{p(d, d_g, \sigma_g)}{\max(p(d, d_g, \sigma_g))} \\
p(d, d_g, \sigma_g) &= \frac{1}{\sqrt{2\pi} d \ln \sigma_g} \exp\left( -\left( \frac{\ln(d/d_g)}{\sqrt{2} \ln \sigma_g} \right)^2 \right)
\end{aligned}
\tag{1}
$$

In (1), $d_{g1}$ and $d_{g2}$, $\sigma_{g1}$ and $\sigma_{g2}$, and $w_1$ and $w_2$ are the geometric mean particle diameters, the geometric standard deviations, and the weights of the small-size mode, $p_1$, and the large-size mode, $p_2$, respectively. The function $p$ is the standard lognormal function and $p_n$ is the peak-normalized lognormal function. Instead of $p$, $p_n$ is used in the following tests, since it does not change its peak value with $d_g$, making it easier to understand the influence of the weight parameter, $w$, and the geometrical mean diameter, $d_g$, separately. It should be noted, that even if $\sigma_g$ is fixed, the standard deviation of $p_n$ becomes larger with larger $d_g$, which is also common for experimental data [27, 29].

The bimodal distribution has been constructed in such a way that the weights $w_1$ and $w_2$ are the values of the peaks of the small-size mode, $p_1$, and the large-size mode, $p_2$, respectively. When the modes overlap, the positions of the peaks of the bimodal distribution become slightly shifted from the peaks of the modes when viewed separately. When the distance between the modes becomes smaller, leading to a stronger overlap, the combined shape of the two modes forms a distribution where the individual peaks gradually disappear. Still, in this theoretical work, we use the definition bimodal for such distributions, as they are obtained using two separate lognormal functions.

## 3 Results and discussion

### 3.1 Evaluation of an experimental size distribution

The size distribution A in Table 1 was used as input data to the LII model to simulate an LII signal, which was then evaluated as if it was originating from a unimodal lognormal distribution. The original and evaluated size distributions are shown in Fig. 1. The lognormal parameters of the evaluated distribution are $d_{g2} = 10.8$ nm and $\sigma_{g2} = 1.35$. It is shown that the evaluated unimodal distribution is similar to the large-size mode of the bimodal distribution, both in position and shape, and that it is slightly shifted towards the small-size mode. Since LII is more sensitive to the larger particles, mainly due to the volume dependence of the signal, this result is not unexpected.

Because fitting of an experimental LII signal using a lognormal size distribution is known to be sensitive to noise and other inaccuracies [12], it can be informative to fit a modeled LII signal based on a monodisperse size distribution to the simulated LII signal. Even if size distributions are not monodisperse in reality, the evaluated particle diameter gives a rough estimate of the particle sizes in the probe volume, which can be sufficient in some cases. The monodisperse fit to the simulated LII signal from the bimodal lognormal distribution is shown in Fig. 1, and gave the result $d = 14.8$ nm. As expected, the fitted monodisperse size distribution is biased towards the larger particle sizes within the bimodal lognormal distribution [31]. To see the influence from the small-size mode on the monodisperse fit, a monodisperse fit was also done for an LII signal simulated from just the large-size mode of the bimodal lognormal distribution. It has not been plotted in the figure, since it differs with less than 0.5% from the result of the fit to the bimodal distribution. This very small difference is attributed to the relative insensitivity to smaller particles of the LII measurement method.

To assess the influence of the heat accommodation coefficient, $\alpha_T$, and the absorption function, $E(m)$, on the calculated values, these parameters were varied in the intervals

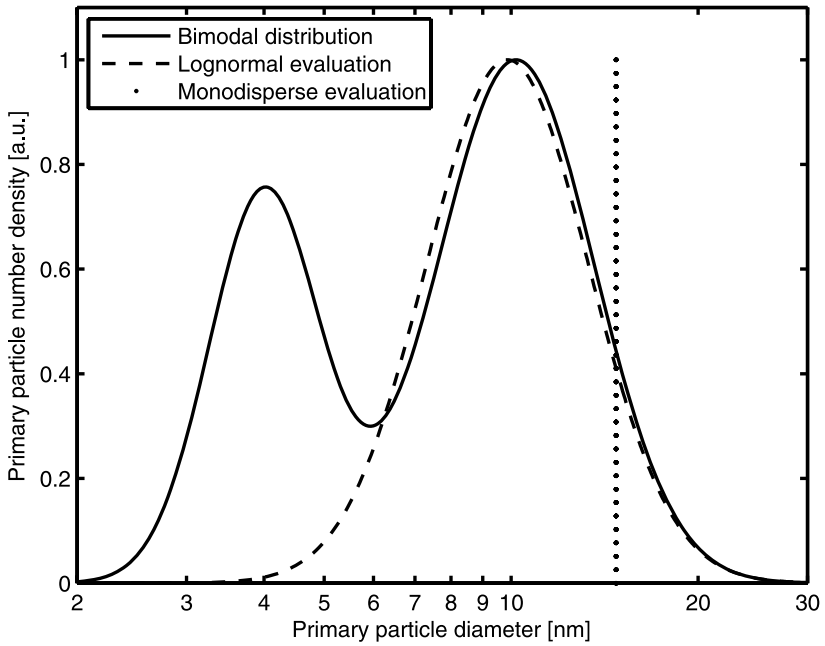


**Fig. 1** The *solid curve* shows the bimodal lognormal distribution A from Table 1, where the large-size mode parameters are $d_{g2} = 11.1$ nm and $\sigma_{g2} = 1.34$. The *dashed curve* shows the lognormal distribution, found by evaluating a simulated LII signal from the bimodal distribution, with $d_{g2} = 10.8$ nm and $\sigma_{g2} = 1.35$. The position of the evaluated monodisperse size is shown by the *dotted line*, with $d = 14.8$ nm. This evaluated monodisperse size was the same (within 0.5%) if only the large-size mode was used to simulate the LII signal. All evaluations started 20 ns after the peak of the signal

$\alpha_T = 0.2$–$0.6$ and $E(m) = 0.3$–$0.5$. Their influences on the lognormal evaluation were found to be negligible: the maximum deviations from the results above were below 0.5% for $d_g$ and below 0.2% for $\sigma_g$. Additionally, varying the detection wavelength resulted in negligible influence on the evaluated size distribution.

### 3.2 Influence of size and position of the small-size mode

The tests of the influence of the small-size mode in a bimodal lognormal distribution in the previous section were made for a certain distribution similar to one that was measured experimentally. To assess the influence of a wider variety of bimodal distributions on the evaluated sizes, signals from bimodal lognormal distributions were first simulated using the LII model, with the parameters shown in Table 1, case B. The large-size mode was fixed at $d_{g2} = 11.0$ nm and $\sigma_{g2} = 1.3$, and the geometric standard deviation of the small-size mode was fixed at $\sigma_{g1} = 1.3$. These values were chosen to be similar to the distribution tested in the previous section, but since $\sigma_g$ shows relatively small variations in sooting flames, the geometrical standard deviation was fixed at the same value to simplify the analysis of the results. Since only the relative weights of the modes are relevant when evaluating the shape of the size distribution, in this test the peak value of the large-size mode, $w_2$, is always set to one. The ranges of the weight of the small-size mode ($w_1$) and geometric diameter ($d_{g1}$) in Fig. 2 were chosen to approximately cover the ranges found in [27] and [29]: $w_1 = 0$–$10$ and $d_{g1} = 3.0$–$11.0$ nm.

The LII signal simulated from the bimodal distribution was first evaluated with the assumption that it was originating from a monodisperse distribution. The monodisperse case was tested since it is the most simple type of evaluation, with only one size parameter in the fit, $d_e$, instead of two, $(d_g, \sigma_g)$, for the lognormal distribution. The evaluated monodisperse size, called the monodisperse equivalent size, was plotted as a function of the geometric mean diameter, $d_{g1}$, and the weight, $w_1$, of the small-size mode of the bimodal distribution, in Fig. 2a. Before discussing the features of Fig. 2a, it should be noted that the monodisperse evaluation will result in a diameter of 14.0 nm if the small-size mode is not present. It is this value that the data in Fig. 2a should be compared to.

There are two features that can be immediately observed in Fig. 2a. Firstly, if the geometrical mean diameter of the small-size mode, $d_{g1}$, is kept constant, increasing the weight $w_1$ of the small-sized mode results in a decrease in the evaluated monodisperse diameter, independent of which $d_{g1}$ is chosen. This is obviously the effect of the smaller particles getting more influence on the shape of the signal decay as $w_1$ is increasing. Secondly, keeping $w_1$ constant and decreasing $d_{g1}$, starting with $d_{g1}$ equal to the geometric mean of the large-size mode, initially results in a decrease in evaluated monodisperse size. This is because the contributions of the two modes to the signal are of similar magnitude, meaning that as the mean of the small-size mode decreases, it will initially pull the monodisperse equivalent size towards smaller values. However, the strength of the signal originating from the small-size mode decreases with $d_{g1}$, due to its smaller volume fraction and shorter decay time, meaning that the influence of the small-size mode on the signal eventually will become so small that the evaluated size starts to increase, once again approaching the monodisperse equivalent size of the large-size mode. At the turning point there is a mini-

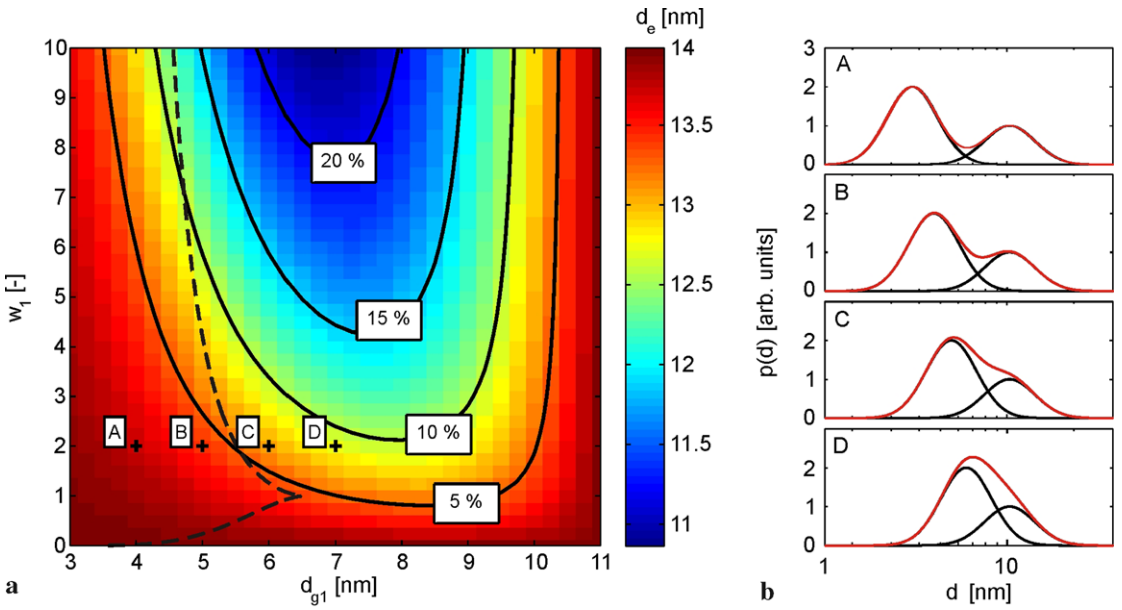


**Fig. 2** (**a**) The monodisperse size evaluated from LII signals simulated from bimodal lognormal distributions with different values of $d_{g1}$ and $w_1$. For the bimodal distributions, the parameters of the large-size modes are fixed at $d_{g2} = 11.0$ nm and $\sigma_{g2} = 1.3$, while only the geometrical width of the small-size modes is fixed, $\sigma_{g1} = 1.3$. The *solid black lines* are contour lines showing the deviation from the evaluated monodisperse size of the large-size mode. The *dashed black line* shows where the minimum in between the peaks of the bimodal distribution disappears when moving from left to right in the figure. (**b**) Plots A–D show how the shape of the bimodal distribution changes when $w_1 = 2$ and $d_{g1}$ increases as shown in (**a**). In each plot the individual modes are shown as well as the total size distribution

mum evaluated diameter that depends on $w_1$. Larger values of $w_1$ will result in a smaller minimum evaluated equivalent diameter, and this minimum will appear for smaller values of $d_{g1}$ the larger $w_1$ is. By analyzing the figure in more detail, it can be stated that if the weight of the small-size mode is less than 75% of that of the large-size mode, the monodisperse equivalent size is at most 5% lower than that evaluated for the large-size mode only. If the weight of the small-size mode is less than 200% of that of the large-size mode, the monodisperse equivalent size is at most 10% lower.

The bimodal distributions marked in Fig. 2a as A, B, C and D, with $w_1 = 2$ and different $d_{g1}$, are shown in Fig. 2b. In distribution A the two peaks are clearly recognizable, but they are gradually moved closer to each other in B and C, and they form a single peak in D. The dashed black line in Fig. 2a marks the limit where the local minimum in between the two peaks in the bimodal distribution disappears when $d_{g1}$ is increased.

When evaluating the bimodal signal using a unimodal lognormal distribution with geometrical mean diameter, $d_g$, and geometrical standard deviation, $\sigma_g$, the results are similar to the case when evaluating using a monodisperse distribution. The graph for $d_g$, equivalent to Fig. 2a, appears similar to that of the monodisperse equivalent size, $d_e$, while $\sigma_g$ tends to get slightly larger values when the weight of the small-size mode is increased.

### 3.3 Influence of the start time of evaluation

It was demonstrated in Fig. 1 that the evaluation of a bimodal size distribution using a lognormal size distribution to a large extent corresponds to the large-size mode of the distribution. A question that arises is if the experimental arrangement or theoretical analysis can be adjusted so that the evaluated lognormal size distribution even more resembles the large-size mode of the distribution. As has been previously mentioned, the contribution of smaller particles in a size distribution to the LII signal becomes smaller for longer times from the particle heating due to their higher cooling rate. This means, that when evaluating a polydisperse particle size distribution as if it were monodisperse, the evaluated particle size will depend on which part of the signal that is used for the evaluation. A later start time for the analysis thus means smaller influence from the small-size mode.

To investigate the influence of the start time of the evaluation, the monodisperse equivalent size was calculated for the bimodal distribution A in Table 1, for different values of the start time, as shown in Fig. 3. It is shown that the monodisperse equivalent size becomes larger the further from the peak of the signal the evaluation starts, which is expected since the smaller particles then get less influence on the signal. Thus a delayed start of evaluation will decrease the influence of the small mode resulting in evaluated sizes closer to the large size of a bimodal distribution. However, the

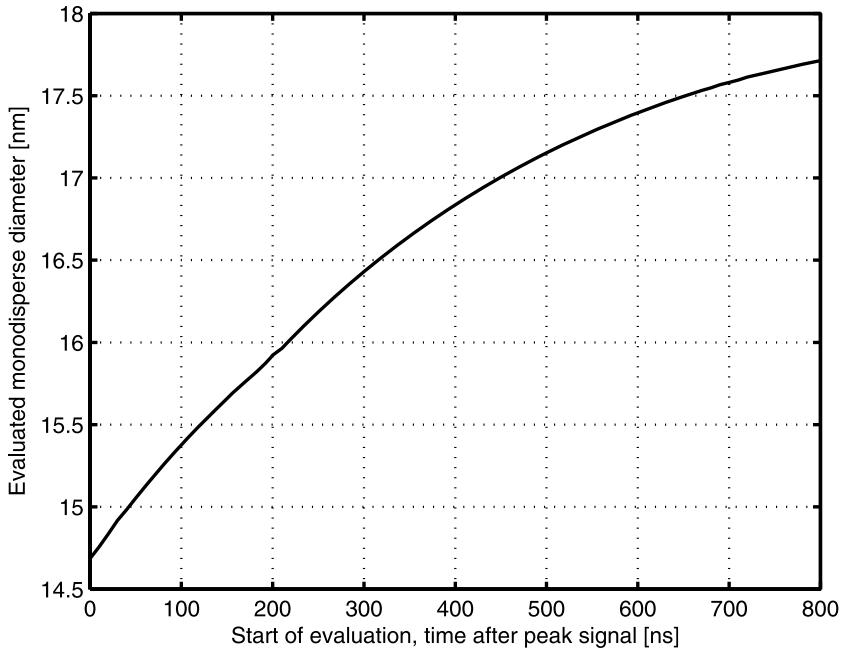


**Fig. 3** The evaluated monodisperse equivalent size of the bimodal distribution specified in Table 1, case A, as a function of the start time of the evaluation (after peak signal value). The monodisperse equivalent size increases with start time since the influence of the smaller particles in the bimodal distribution decreases with time. The total signal length from time of peak was 900 ns

scheme does at the same time increase uncertainties as a result of increasing influence of noise when relying on later parts of the LII signals, making the scheme unsuitable for many experimental investigations.

### 3.4 Influence of different particle properties of the two modes

One assumption in the present work is that the particles in the two modes of a bimodal size distribution have the same properties. This assumption is apparently questionable for the bimodal distributions observed in the nucleation and growth region of premixed flat flames [27, 29, 32], since it is well known that particles undergo changes in morphology, chemical composition, and optical properties. These changes may influence the heating and cooling rates of the particles when using LII. For example, it can be expected that the smaller particles close to the sizes where particle nucleation occurs are more transparent [32, 33], meaning that particle temperatures become lower and their contribution to the total LII signal smaller than what the theoretical investigation shows. Recent experimental findings in our own group indicate that particles at lower heights in a flat sooting premixed flame are heated to lower temperatures for constant laser fluence [34]. This may be interpreted as originating from a variation in $E(m)$ as a function of height, but also variations in the physical properties of the particles, like their density and heat capacity will influence the results. Another assumption is that the particles independent of size can be heated to temperatures up to 3600 K. Soot is considered to mainly be a disordered graphite structure, and graphite has a sublimation temperature of 3915 K [35]. Since graphite is one of the substances with the highest sublimation temperature it is plausible that a smaller particle with less graphitic structure and higher hydrogen content has a lower sublimation temperature. Following this argumentation, the contribution from the small-size mode in a real experimental situation will most probably be less than what the theoretical investigations in this paper show.

## 4 Conclusions

The simulated LII signal from bimodal lognormal primary particle size distributions was evaluated using a model for LII, assuming the signal originated from a monodisperse or a unimodal lognormal distribution. It was generally found that the small-size mode has relatively little influence on the evaluated particle size.

A parameter study was made, by finding the monodisperse equivalent particle size of a bimodal lognormal size distribution for a range of different weights and positions of the small-size mode. The estimated monodisperse equivalent size was relatively insensitive to the size and position of the small-size mode. If the weight of the small-size mode is less than 75% of that of the large-size mode, the monodisperse equivalent size is at most 5% lower than that evaluated for the large-size mode only. If the weight of the small-size mode is less than 200% of that of the large-size mode, the monodisperse equivalent size is at most 10% lower.

The evaluation start time of a time-resolved LII signal was varied, and it was shown that monodisperse evaluations of signals from bimodal lognormal distributions resulted in larger particle sizes when the start position was delayed.

A delay of the start position for the evaluation suppresses the impact of the smaller particles with faster signal decay. However, such procedures should be made with caution since reliable size evaluations will become increasingly difficult as the signal-to-noise ratio becomes lower at later times.

**Acknowledgements** This work is funded by the Swedish Research Council and the Swedish Foundation for Strategic Research (SSF) where it is part of the Transient Spray project within the CECOST program.

## References

1. R.J. Santoro, C.R. Shaddix, in *Applied Combustion Diagnostics* (Taylor & Francis, New York, 2002), p. 252
2. C. Schulz, B.F. Kock, M. Hofmann, H. Michelsen, S. Will, B. Bougie, R. Suntz, G. Smallwood, Appl. Phys. B **83**, 333 (2006)
3. R.W. Weeks, W.W. Duley, J. Appl. Phys. **45**, 4661 (1974)
4. A.C. Eckbreth, J. Appl. Phys. **48**, 4473 (1977)
5. S. Will, S. Schraml, K. Bader, A. Leipertz, Appl. Opt. **37**, 5647 (1998)
6. R.L. Vander Wal, T.M. Ticich, A.B. Stephens, Combust. Flame **116**, 291 (1999)
7. S. Schraml, S. Dankers, K. Bader, S. Will, A. Leipertz, Combust. Flame **120**, 439 (2000)
8. B. Axelsson, R. Collin, P.-E. Bengtsson, Appl. Opt. **39**, 3683 (2000)
9. B. Axelsson, R. Collin, P.-E. Bengtsson, Appl. Phys. B **72**, 367 (2001)
10. T. Lehre, H. Bockhorn, B. Jungfleisch, R. Suntz, Chemosphere **51**, 1055 (2003)
11. S. Dankers, A. Leipertz, Appl. Opt. **43**, 3726 (2004)
12. K.J. Daun, B.J. Stagg, F. Liu, G.J. Smallwood, D.R. Snelling, Appl. Phys. B **87**, 363 (2007)
13. B.F. Kock, B. Tribalet, C. Schulz, P. Roth, Combust. Flame **147**, 79 (2006)
14. H.A. Michelsen, P.O. Witze, D. Kayes, S. Hochgreb, Appl. Opt. **42**, 5577 (2003)
15. H.A. Michelsen, F. Liu, B.F. Kock, H. Bladh, A. Boiarciuc, M. Charwath, T. Dreier, R. Hadef, M. Hofmann, J. Reimann, S. Will, P.-E. Bengtsson, H. Bockhorn, F. Foucher, K.P. Geigle, C. Mounaïm-Rousselle, C. Schulz, R. Stirn, B. Tribalet, R. Suntz, Appl. Phys. B **87**, 503 (2007)
16. H. Bladh, J. Johnsson, P.-E. Bengtsson, Appl. Phys. B **90**, 109 (2008)
17. S. Will, S. Schraml, A. Leipertz, Proc. Combust. Inst. **26**, 2277 (1996)
18. S. Will, S. Schraml, A. Leipertz, Opt. Lett. **20**, 2342 (1995)
19. P. Roth, A.V. Filippov, J. Aerosol Sci. **27**, 95 (1996)
20. Ü.Ö. Köylü, G.M. Faeth, Combust. Flame **89**, 140 (1992)
21. T. Lehre, B. Jungfleisch, R. Suntz, H. Bockhorn, Appl. Opt. **42**, 2021 (2003)
22. M. Hofmann, B.F. Kock, T. Dreier, H. Jander, C. Schulz, Appl. Phys. B **90**, 629 (2008)
23. H. Bladh, J. Johnsson, P.-E. Bengtsson, Appl. Phys. B **96**, 645 (2009)
24. K. Tian, F.S. Liu, K.A. Thomson, D.R. Snelling, G.J. Smallwood, D.S. Wang, Combust. Flame **138**, 195 (2004)
25. S. Banerjee, B. Menkiel, L. Ganippa, Appl. Phys. B **96**, 571 (2009)
26. C.F. Bohren, D.R. Huffman, *Absorption and Scattering of Light by Small Particles* (Wiley, New York, 1998)
27. R. Stirn, T.G. Baquet, S. Kanjarkar, W. Meier, K.P. Geigle, H.H. Grotheer, C. Wahl, M. Aigner, Combust. Sci. Technol. **181**, 329 (2009)
28. M.M. Maricq, S.J. Harris, J.J. Szente, Combust. Flame **132**, 328 (2003)
29. A.D. Abid, N. Heinz, E.D. Tolmachoff, D.J. Phares, C.S. Campbell, H. Wang, Combust. Flame **154**, 775 (2008)
30. T. Lehre, Ph.D. Thesis. University of Karlsruhe (2005)
31. H. Bladh, P.-E. Bengtsson, Appl. Phys. B **78**, 241 (2004)
32. A. D'Anna, Proc. Combust. Inst. **32**, 593 (2009)
33. T.T. Charalampopoulos, J.D. Felske, Combust. Flame **68**, 283 (1987)
34. H. Bladh, J. Johnsson, N.-E. Olofsson, A. Bohlin, P.-E. Bengtsson, in *33rd International Symposium on Combustion in Beijing* (2010, submitted)
35. H.R. Leider, O.H. Krikorian, D.A. Young, Carbon **11**, 555 (1973)